Efficient H_2 production by photocatalytic water splitting under UV or solar light over variously modified TiO_2-based catalysts

R. Fiorenza[1,2], **S. Sciré[1*]**, L. D'Urso[1], G. Compagnini[1],
M. Bellardita[3], L. Palmisano[3]

[1] *Dipartimento di Scienze Chimiche, Università di Catania, Viale Andrea Doria 6, 95125 Catania, (Italy).*

[2] *CNR-IMM, Via Santa Sofia 64, 95213 Catania, (Italy).*

[3] *Dipartimento di Ingegneria, Università di Palermo, Viale delle Scienze, 90128 Palermo (Italy).*

*** Corresponding author**

Phone:+39/0957385112

Fax:+39/095580138

e-mail address: sscire@unict.it

Keywords: Hydrogen, Titania, Ceria, Tungsten, Laser treatment, Macroporous structure.

Abstract

This paper focuses on different modification strategies to adjust the chemico-physical properties of TiO_2-based photocatalysts exploring the results of the modifications on H_2 production by water splitting under UV or simulated solar irradiation. The results over variously modified TiO_2 based catalysts were compared and rationalized in order to discriminate among the key features involved in the photocatalytic H_2.

First approach considered the use of pulsed laser irradiation (LT) of aqueous TiO_2 suspensions to induce structural transformations on the bulk and the surface of anatase TiO_2. In this case a great increase of the water splitting activity was found under UV light and this was related to the presence of Ti^{3+} defects and oxygen vacancies in the TiO_2 structure. The second strategy was based on a templating method to obtain TiO_2 with a macroporous structure (Macro-TiO_2), which results in an efficient light absorption process inside the material pores, leading to higher H_2 production, mainly when working under solar light irradiation. The third method consisted in the coupling of TiO_2 or Macro-TiO_2 with CeO_2 as host components, or W as doping agent. It was found that this approach strongly enhanced the TiO_2 photoactivity mainly under solar light irradiation, with CeO_2 acting as a photosensitizer and W as doping agent inducing defects formation.

Graphical abstract

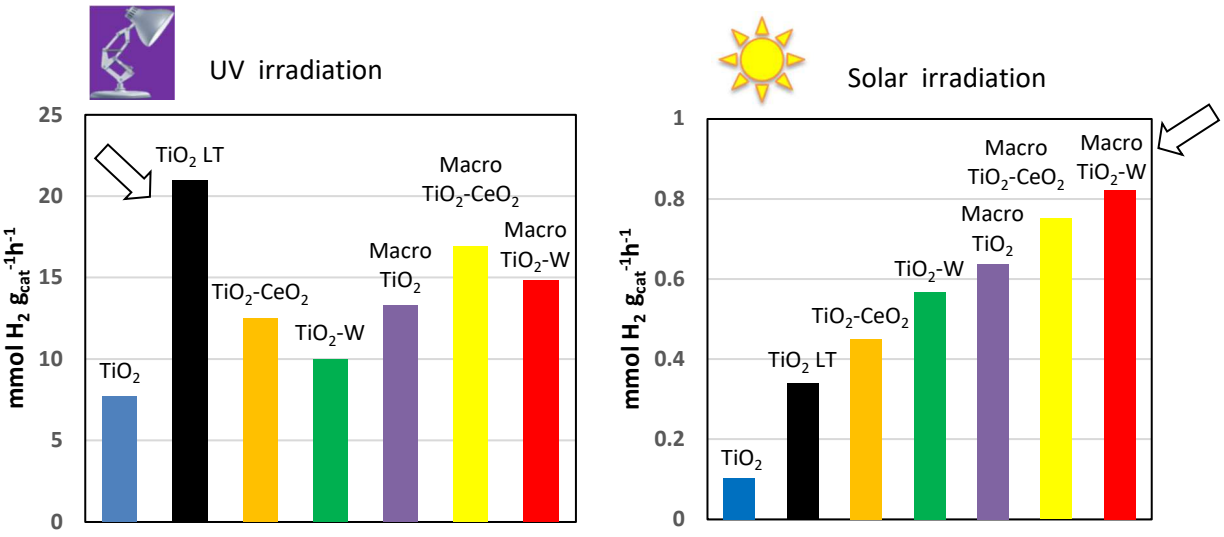

1. Introduction

The rapid growth over the past century of a large-scale economy and industrialization has given rise to serious concerns regarding both the depletion of natural resources and the global warming. Despite these troubles, fossil fuels still remain the major source of energy in people's daily life. This has prompted the research toward clean renewable energy sources.

After its first application in water cleavage, with hydrogen production using a TiO_2 photoanode in 1972 [1], photocatalysis attracted an immediate interest, because of the 1973 and 1979 energy crises. Since then, the attention of the scientific community raised continuously in so as photocatalysis represents the ideal green technology which uses a renewable and available energy resource as solar light and mild reaction conditions. Photodegradation of pollutants and production of clean fuels by photocatalytic water splitting or CO_2 photoconversion were the hottest subjects in photocatalysis [2-4].

Since its appearance on the market in the early 20th century, titanium dioxide (TiO_2) underwent an extensive use in several applications (sunscreens, paints, ointments, toothpaste, etc). Moreover after the first report in 1972 by Fujishima and Honda [1], TiO_2 has been largely employed in solar cells, lithium, biomedical devices and at present is by far the most used photocatalyst exploiting its non-toxicity, good stability and low cost [5-7]. However, there are still some inherent disadvantages restraining the wide use of TiO_2 in the various photocatalytic applications. In fact, due to the wide band gap (3.2 and 3.0 eV for anatase and rutile, respectively) TiO_2 suffers a low exploitation of the solar electromagnetic spectrum. Moreover, a fast recombination of photo-produced electron-hole pairs and a large overpotential for the splitting of water leads to low photoefficiency. Therefore, in the last years, several efforts have been pursued in order to enhance the TiO_2 photoefficiency, aiming to expanding the photocatalytic surface, giving rise to Schottky junctions or heterojunctions, and tailoring the structure of bands to match specific energy levels with structural or chemical modifications [8-10].

In this paper we compared different strategies that we have applied to adjust the chemico-physical properties of TiO_2 pointing out the specific role of each of these changes on the photocatalytic performance in the H_2 production by water splitting either under UV or solar light irradiation. Specifically: a) we induced structural changes in the surface and bulk TiO_2 by laser treatment in water, an easy and green method to obtain reduced highly photoactive TiO_2 species [11], b) we used a template strategy to get TiO_2 with a highly ordered macroporous structure (Macro-TiO_2) [12], and c) we performed chemical modifications of both anatase TiO_2 and Macro-TiO_2 by the addition of a host component (CeO_2), acting as photosensitizers, or a doping agent (W), introducing defects [13].

2. Experimental

2.1 Catalysts preparation

Concerning with untreated oxides used in this work, TiO_2 was commercial anatase (Sigma Aldrich, prod. Nos. 637254) and CeO_2 was home synthesized by KOH (0.1 M) precipitation from $Ce(NO_3)_3 \cdot 6H_2O$ aqueous solution as reported in refs. [14,15].

Anatase TiO_2-10 wt.% CeO_2 composite (coded TiO_2-CeO_2) and anatase TiO_2-10% at. W (coded TiO_2-W) were prepared by wet-impregnation using the proper amount of $Ce(NO_3)_3 \cdot 6H_2O$ and tungsten (VI) chloride as metal salt precursor, then stirring the slurry for 3 h, drying in an oven at 100°C for 24 h and treating in air at 350°C for 3 h.

For laser treated samples (TiO_2 LT), TiO_2 was dispersed in distilled water and sonicated, then irradiated under stirring using the second harmonic radiation (532 nm) of a Nd:YAG nanosecond pulsed laser. Details of the laser system, the beam and the irradiation conditions were reported in ref [11].

Macroporous TiO_2 (coded Macro-TiO_2) was synthesized by adopting the templating strategy reported in refs [12-13]. Briefly, polystyrene (PS) spheres (300 nm) were impregnated by drop-wise addition of titanium isopropoxide. The precursor-template mixture was then dried for 24 h and treated in air at 550°C for 12 h. Macroporous anatase TiO_2-10wt.% CeO_2 composite (coded Macro-TiO_2-CeO_2) was prepared by wet-impregnation of Macro-TiO_2 using the appropriate amount of $Ce(NO_3)_3 \cdot 6H_2O$, followed by 100°C drying for 24h and 350°C air treating for 3h. Macroporous TiO_2-10at.% W (coded Macro-TiO_2-W) was prepared with the same procedure of bare Macro-TiO_2 adding titanium isopropoxide and a proper amount of tungsten (VI) chloride.

2.2 Catalysts Characterization

The structure, the morphology and the texture of samples were evaluated by a) scanning electron microscopy (SEM) ~~using~~ with a Jeol JSM-7500F microscope; b) X-ray powder diffraction (XRD) with a Bruker AXSD5005 diffractometer (Cu Kα radiation), comparing peaks with the JCPDS database; c) adsorption-desorption of N_2 at -196°C using a Sorptomatic series 1990 (Thermo Quest) with prior overnight outgassing of samples at 120°C.

The characterization of the optical behaviour was carried out by: a) a WITec alpha 300 confocal Raman apparatus exciting with a 532 nm laser line of a Coherent Compass Sapphire Laser; b) Ultraviolet-Visible-Diffuse Reflectance Spectroscopy (UV-Vis DRS) in the range of 200-800 nm using a Jasco UV-visible spectrometer, with a Labsphere for diffuse reflectance

analysis, and $BaSO_4$ as the reference; c) Photoluminescence (PL), using a Perkin Elmer LS45 apparatus and 320 nm as the excitation wavelength.

2.3 Photocatalytic activity tests

Photocatalytic water splitting test runs were carried out in a jacketed Pyrex reactor, kept at 30°C, and by irradiating the suspension of the catalyst (25 mg) in deionized water (45 ml)-ethanol (5 ml, used as sacrificial agent) with a 100 W UV mercury lamp (Blak-Ray B 100A, 365 nm) or with a 300W sunlight simulating lamp (Osram Ultra Vitalux). Prior to irradiation the stirred suspension was purged 1 h in Ar to get rid of dissolved air. H_2 evolution was determined by an online gas chromatograph supplied with Carboxen 1000 packed column and thermal conductivity detector working with Ar as carrier gas.

3. Results and discussion

As discussed in the introduction chapter of this paper, we applied different strategies in order to modify properties of anatase TiO_2 and to assess the role of the changes on the photocatalytic H_2 generation by water splitting either under UV or solar light.

3.1 Laser treatment in water

Reduced TiO_2 (TiO_{2-x}) materials, also known as black titania, have received considerable attention in the last years, on account of the high photocatalytic and photoelectro-chemical performance [11, 16], caused by peculiar properties such as broadened absorption in the solar light region, surface and bulk structural changes with creation of Ti^{3+} species and oxygen vacancies. The most used methods to reduce TiO_2 (thermal treatment in H_2 flow, treatment under vacuum, or using hydrogen plasmas) entail high temperatures (400–700°C), the use of vacuum arrangement and multistep procedures with long processing times. Here we considered an alternative, easy and green approach to obtain reduced TiO_2 by laser irradiation in aqueous dispersion [11, 17]. According to the above literature, laser treatment of anatase TiO_2 determined significant structural modifications of the TiO_2, as confirmed by the characterization techniques used (Raman and PL), which are gathered in Fig. 1 for TiO_2, TiO_2 LT and Macro TiO_2 samples, and by an indirect qualitative indication as the slight grey/blue coloration of the treated sample.

In particular the Raman characterization (Fig. 1A) clearly show similar spectra for TiO_2 and Macro-TiO_2 samples, pointing to the presence of the typical features of anatase, namely a main band at 140 cm^{-1} (E_g), due to the O-Ti-O vibration, and three other ones at 395 cm^{-1} (A_{1g}), 515 cm^{-1} (B_{1g}) and 635 cm^{-1} (E_g). It can be noticed that the laser irradiation treatment in

water causes a partial crystalline phase change from anatase to rutile, as demonstrated by the appearance of the bands at 445 and 600 cm^{-1} in the TiO_2 LT sample, distinctive of rutile (E_g). This is also well discernible in the Raman maps reported in Fig. 1B showing in blue the signals at 140 cm^{-1} for anatase and in red those at 445 cm^{-1} for rutile. A similar trend of partial phase transformation (anatase → rutile) has been already reported by some of us in the case of laser treatment of TiO_2 P25 [11].

In Fig. 1C PL spectra of TiO_2, TiO_2 LT and Macro TiO_2 samples are abridged. It can be seen that for all three samples the spectrum is quite broad, with several components in the 350-600 nm range, reasonably related to the typical PL features of anatase titania, namely at 370-390 nm (band to band emission of the TiO_2 [18]), 430 (self-trapped excitons confined on TiO_6 octahedral [19]), 475, 525 and 560 nm (electrons in defective Ti centres connected with oxygen vacancies [20]). Interestingly the TiO_2 LT sample exhibits a spectrum with a significant higher intensity in the 450-600 nm region, pointing to a higher number of defects, whose number has been reported to be somewhat correlated to the PL intensity in this region [20-22].

The band gap energies values for the investigated samples, calculated using the modified Kubelka-Munk spectral function $[F(R_\infty')h\nu]^{1/2}$ on the basis of UV-vis DRS spectra are displayed in Table 1. No substantial variations of the E_g values were calculated for TiO_2, TiO_2 LT and Macro TiO_2 samples.

On account of the above characterization it can be concluded that laser treatment of TiO_2 results in the introduction of lattice distortion with Ti^{3+} species and oxygen vacancies and in a moderate change in the crystal phase of TiO_2 with a small increase in the BET surface area (Table 1). These changes probably concur to the relevant enhancement of the photoactivity of TiO_2 LT with a significant increase of H_2 production by photocatalytic water splitting, especially under UV irradiation (Fig. 2). The occurrence of defects in the crystalline structure of TiO_2 is the key factor explaining the increase of the H_2 production. The defects, in fact, act as hole traps owing to the creation of a Ti^{3+} donor level just below the bottom of the CB [11], thus strongly decreasing the recombination rate between the photoholes and the electrons.

3.2 Templating strategy and chemical modifications

The second approach was based on the combination of a template strategy, aimed to obtain TiO_2 with a macroporous structure (Macro TiO_2), and chemical modifications achieved by adding CeO_2 as host component or W as doping agent.

TiO_2 catalysts with macro-mesoporous structures have attracted the interest of the researchers working in heterogeneous photocatalysis due to the highly available surface area

and the regular size of the pores with intrinsic connectivity, which help both efficacious charge transfer and reactants mass flow [23]. The higher photoactivity of these systems was attributed to the specific porous structure of TiO_2 leading to a high efficient light absorption process inside the material pores [12, 13, 24, 25]. In Fig. 3 the SEM images, at the same magnification, of Macro TiO_2, Macro TiO_2-CeO_2 and Macro TiO_2-W are reported. It can be seen that all macroporous TiO_2-based samples have a specific porous macrostructure made of interconnected cavities. This is in accordance with the lower surface area of these latter samples (23-28 m^2/g vs. 55-61 m^2/g of the non-Macro TiO_2 samples) as shown in Table 1.

Interestingly the Macro TiO_2 sample was more active than TiO_2 in the H_2 production (Fig. 2). In particular the activity enhancement effect of the macroporous TiO_2 was much higher under simulated solar than UV light irradation. In fact, Macro TiO_2 exhibited 2 and 6 times higher H_2 production than the anatase TiO_2 sample under UV and solar light, respectively. While the Raman spectra of TiO_2 and Macro TiO_2 are similar (Fig.1A), the Macro TiO_2 shows instead a PL spectrum more intense than the TiO_2 one in the band to band emission region (Fig. 1C), pointing to the presence of more excitons species. The highly porous structure, in fact, increases the formation of charge carriers in so as it leads to an easier access and mass transfer allowing light waves to easily enter the photocatalyst [12, 13, 23-25]. This results in an increase of the path length of light and in an improved photoactivity.

3.3 Chemical modification (Doping with CeO_2 or W)

It has been broadly accounted that photocatalytic activity of titania can be strongly affected by coupling TiO_2 with other oxides (ZnO, Cu_2O, Bi_2O_3, $BiVO_4$, CeO_2) [12, 15, 26-28] or doping with metallic (V, W, Fe) [13, 29-31] or non-metallic elements (C, N, S, F) [13, 32-35]. In particular the combination of titania with an appropriate amount of specific oxides (as CeO_2) can be highly beneficial for the photoactivity in so as the oxide can favour the electron transfer from TiO_2 to the other oxide or vice versa, leading to a lower e^-/h^+ recombination rate and therefore to an enhancement of the charge separation [10, 12, 15]. Doping with metallic or non-metallic elements may instead boost the generation of oxygen vacancies, propping up the activity via excitation of electrons from the VB to the oxygen vacancies energy levels [31,36]. In accordance with the above considerations in this work we investigated how CeO_2 or W modified the physicochemical and photocatalytic properties of anatase TiO_2 (TiO_2 sample) and macroporous TiO_2 (Macro TiO_2 sample).

Interestingly, Raman spectra (Fig. 4A) show that chemical treatments with CeO_2 do not significantly affect the distribution and the position of the TiO_2 bands, pointing out that anatase remains the only phase present. It can be noted that ceria-modified samples (TiO_2-

CeO_2 and Macro TiO_2-CeO_2) show an E_g value 0.05 eV lower than anatase TiO_2 and Macro TiO_2, in agreement with previous literature data [10, 12] and ascribed to the substitution of the lattice Ti^{4+} species with Ce^{4+} or Ce^{3+} ones [37, 38].

The addition of tungsten results in a different behaviour depending on the TiO_2 used (TiO_2 or Macro TiO_2). Interestingly, in fact, the Raman spectra of TiO_2-W (Fig. 4A) exhibited two bands at 273 cm^{-1} and 718 cm^{-1} respectively, attributed to vibration modes of orthorhombic WO_3 [39, 40]. In particular, the peak at 270 cm^{-1} is related to the O–W–O bending vibrations of the bridging oxygen, and the peak at 718 cm^{-1} to the corresponding stretching mode. Furthermore, in this latter sample a red shift of the main peak of the anatase phase (at around 150 cm^{-1}) was observed (inset of Fig. 4A). Considering that this band is attributed to the main vibrational mode of anatase (O–Ti–O) [10], the presence of WO_3 in the TiO_2 lattice probably produces a bond distortion which causes the measured shift. However, the above peaks and the red shift of the O–Ti–O band of anatase are not observed in the spectra of Macro TiO_2-W. Reasonably, in this sample the porous backbone of TiO_2 allows a higher dispersion of tungsten with chance of interstitial substitution of titanium by tungsten ions. As reported in the literature [41-43], in fact, tungsten ions can replace Ti^{4+} in the lattice of TiO_2 because of the correspondence of the ionic radius of W^{4+}/W^{6+} and Ti^{4+}. Accordingly, nonstoichiometric solid solution of $W_xTi_{1-x}O_2$ or TiO_2-amorphous WO_x composites would form, with potential generation of tungsten impurity energy levels.

The PL spectra of investigated TiO_2-based catalysts are reported in Fig. 4B. It must be reminded that the bare CeO_2 displays the band to band emission peak at around 455 nm. It can be noted that doping TiO_2 with CeO_2 or W (TiO_2-CeO_2 and TiO_2-W samples) causes an increase of the intensity of the band to band emissions (region at around 375 cm^{-1}) but a decrease in the intensity of bands at higher wavelengths (> 470 cm^{-1}), associated with the recombination rate of charges, thus pointing to a lower recombination rate of electron-hole pairs, in other words to a better charge separation efficiency of the doped samples [20-22]. The combination of ceria or W with the Macro TiO_2 (Macro TiO_2-CeO_2 and Macro TiO_2-W samples) caused a drop of the intensity of all of the bands. This indicates a restrained radiative recombination process in the Macro TiO_2 doped sample [44], which can be attributed to a change of the defective state at a thin level of the Macro TiO_2 surface [45], probably due to a synergistic effect of the doping and the photonic effect (light harvesting) of macroporous TiO_2. These features enhance the chance of interfacial transport of photo-induced electrons and holes favouring a higher photo-activity [44-46]. The presence of tungsten didn't change the band-gap extension of TiO_2 (Table 1).

The observed changes in the TiO_2 structure due to the coupling with CeO_2 or W have a key importance to interpret the improvement of the photocatalytic activity of this mixed oxide system for the water splitting. In fact, the photoactivity of ceria- or W-doped TiO_2 samples as for H_2 production through water splitting (Figs. 5 and 6) was found to be enhanced both for non-macroporous (Fig.5) and, even more, for macroporous (Fig.6) TiO_2 modified samples. In both cases the extent of this effect appears more relevant under solar light than under UV irradiation. Therefore applying a mixed approach, consisting in modifying TiO_2 or Macro TiO_2 with CeO_2 or W, appears highly effective in the enhancement of the titania photoactivity. In this case the introduction of shallow level defects in a macroporous structure contemporaneously boosts up the light absorption ability and the electron-hole charge disjointing of TiO_2 thus favouring the water reduction for which CB electrons are crucial. Noteworthy regarding the non-macroporous TiO_2 samples, the most important effects can be observed mainly under solar light irradiation, with an H_2 production of about 4 and 6 times higher with TiO_2-CeO_2 and TiO_2-W compared to the bare TiO_2. In the case of UV irradiation the modifications with cerium oxide and tungsten lead to have comparable performances being the H_2 production 12.5 and 10 $mmol \cdot h^{-1} \cdot g_{cat}^{-1}$ with TiO_2-CeO_2 and TiO_2-W, respectively, anyhow higher than the un-modified TiO_2 sample (7.7 $mmol \cdot h^{-1} \cdot g_{cat}^{-1}$).

3.4 General comparison of data and discussion

Fig. 7 summarizes the comparison of the results obtained in this work in terms of H_2 production by photocatalytic water splitting carried out at the same experimental conditions under UV (Fig. 7A) and simulated solar (Fig. 7B) irradiation over the representative TiO_2-based catalysts used. It can be easily observed that under UV light (Fig. 7A), the TiO_2 sample treated by laser ablation in liquid (TiO_2 LT) is notably the most active one, with H_2 generation rate almost triple than that of the untreated sample and about twice those of the other two modified TiO_2-based catalysts (TiO_2-CeO_2 and TiO_2-W).

On the basis of the characterization data, laser treatments lead to a more defective titania sample with the growth of Ti^{3+} and oxygen vacancies. The formation of under-coordinated titanium ions, the stimulated lattice distortion together with the moderate increase of surface area and the formation of rutile phase (see Raman spectra) are the key factors to explain the higher H_2 production under UV irradiation compared to the other modified samples. The under-coordinated Ti ions act, in fact, as anchored and charge injection/recombination sites, changing in a decisive way the electrons/holes recombination dynamics and favouring an easier reduction of proton from water [47,48]. The H atoms will replace the locations of oxygen vacancies in the TiO_2 crystalline structure, thus attracting the electrons from the

nearby Ti and O atoms, resulting in an enhanced H_2 production [49-51]. Reasonably, these effects influence the photocatalytic performance mainly under UV irradiation. In fact, considering that the E_g value of TiO_2 LT is comparable to that of the bare TiO_2 (Table 1), the formation of photoelectrons was much smaller when the reaction was performed under solar than under UV irradiation, even though the laser treatment can induce mid-gap states within the band gap of TiO_2 [52]. Moreover, it cannot be excluded the positive role in the photoactivity played by the contact between the formed rutile phase under laser irradiation and the pre-existing anatase phase [48].

The use of a template strategy to obtain macroporous TiO_2 leads to a raise of the photocatalytic H_2 production of about 1.7 under UV irradiation and 6 times higher under solar irradiation than bare TiO_2. The presence of a macroporous structure enhances the absorption of photons, boosting the optical path length and the transfer rate of electron-hole pairs on the titania surface. This allows an easier H^+ ions reduction on the surface of Macro TiO_2 by the photoproduced electrons [53-55]. This behaviour well agrees with the PL spectrum of the Macro TiO_2, exhibiting a higher intensity of the band due to the excitons (375 nm), according to the higher light adsorption on the macroporous surface and a lower intensity of the bands generally related to the electron-holes recombination rate, as a consequence of the enhanced electron-hole pairs migration rate [12, 13].

The combination of a structural (Macro TiO_2) and a chemical (addition of CeO_2 or W) modification permits to further increase the photoactivity. In particular, with the addition of cerium oxide, the photo-generated electrons can be transferred from CeO_2 to TiO_2 whilst holes, owing to the more positive valence band of TiO_2, can proceed reversely giving rise to an efficacious charge separation and a superior hydrogen production [10, 12, 56]. Moreover, the presence of the Ce^{3+}/Ce^{4+} redox couple gives rise to a scavenging effect in the TiO_2 conduction band further enhancing the charge carrier separation. CeO_2 acts as photosensitizer favouring also a remarkable activity also under solar irradiation. The contemporaneous presence of these effects, namely the macroporous structure with the increase of the light path length and the photosensitizer action of cerium oxide, are essential to rise the hydrogen production with respect to both un-modified TiO_2 and Macro TiO_2 samples.

Interestingly, the Macro TiO_2-W sample is the most active catalyst under solar light irradiation (Fig. 7). As reported in the literature [57-59] tungsten can enter the TiO_2 lattice and partly replace the titanium ions. Moreover, the doping with W can generate new electronic states above the TiO_2 valence band. These new states may facilitate the visible light absorption by TiO_2, thus favouring the activity under solar light irradiation. Similarly to the cerium oxide effect, the addition of tungsten aids in detrapping of charge carriers to the

surface of the photocatalyst, being the energy level of Ti 3d electrons close to that of W 5d electrons [60, 61]. Noteworthy, TiO_2-W and Macro TiO_2-W showed quite different Raman and PL spectra (Fig. 4). Probably, the porous structure promotes the migration of tungsten ions into the crystalline lattice of TiO_2 thus allowing the formation of more electronic states between the valence and the conduction bands of TiO_2. The very low intensity of Macro TiO_2-W PL bands is a further evidence of a higher charge carriers separation. This well agrees with the higher H_2 production observed on the Macro TiO_2-W sample compared to TiO_2 and Macro TiO_2 samples, both under UV and solar light. In the case of the non-macroporous TiO_2 system, the W ions can segregate more easily on the surface of TiO_2 with formation of WO_3 species, pointed out by Raman characterization (Fig. 4A), which can partially block the light absorption process of titania and then contributing to explain the lower photoactivity of TiO_2-W compared to Macro TiO_2-W.

4. Conclusions

On the basis of the results discussed in this paper we can conclude that the induction of structural and chemical modifications of TiO_2 by various approaches is a promising strategy to achieve a more efficient hydrogen production through water splitting over TiO_2-based photocatalysts. The key results of the paper can be summarized as it follows:

a) laser treatment of TiO_2 results in a series of structural changes as introduction of Ti^{3+} species and oxygen vacancies, surface area and crystal phase of TiO_2, which all together concur to the relevant enhancement of the photoactivity of TiO_2 LT sample, specially under UV irradiation.

b) the use of a macroporous ordered structure of TiO_2 leads to slow photon effects with high light absorption, strongly enhancing the TiO_2 photoactivity mainly under solar light irradiation. The positive effect was further increased by the presence of a photosensitizer as CeO_2 or by a doping agents as W, which enhanced the light absorption and the charge separation between electrons and holes of the photocatalyst.

Acknowledgements

Authors would like to thank Giuseppe Francesco Indelli, Laboratory Technician at Bio-Nanotech Research and Innovation Tower, (BRIT) of University of Catania for technical support.

References

[1] Fujishima A, Honda K. Electrochemical photolysis of water at a semiconductor electrode. Nature 1972;238:37-8.

[2] Boyjoo Y, Sun H, Liu J, Pareek VK, Wang S. A review on photocatalysis for air treatment: from catalyst development to reactor design. Chem Eng J 2017;310:537-59

[3] Hisatomi T, Takanabe K, Domen K. Photocatalytic water-splitting reaction from catalytic and kinetic perspectives. Catal Lett 2015;145:95-108.

[4] Li K, An X, Park KH, Khraisheh M, Tang J. A critical review of CO_2 photoconversion: catalysts and reactors. Catal Today 2014;224:3-12.

[5] Fujishima A, Rao TN, Tryk DA. Titanium dioxide photocatalysis. J Photochem Photobiol C 2000;1:1-21.

[6] Schneider J, Matsuoka M, Takeuchi M, Zhang J, Horiuchi Y, Anpo M, Bahnemann DW. Understanding TiO_2 photocatalysis: mechanisms and materials. Chem Rev 2014;114:9919-86

[7] Ohtani B. Titania photocatalysis beyond recombination: a critical review. Catalysts 2013;3:942-53.

[8] Liu G, Wang L, Yang HG, Cheng H-M, Lu GQ. Titania-based photocatalysts-crystal growth, doping and heterostructuring. J Mater Chem 2010;20:831-43.

[9] Chen X, Mao SS. Titanium dioxide nanomaterials: synthesis, properties, modifications and applications. Chem Rev 2007;107:2891-959.

[10] Fiorenza R, Bellardita M, D'Urso L, Compagnini G, Palmisano L, Scirè S. Au/TiO_2-CeO_2 catalysts for photocatalytic water splitting and VOC's oxidation reactions. Catalysts 2016;6:121.

[11] Filice S, Compagnini G, Fiorenza R, Scirè S, D'Urso L, Fragalà ME, Russo P, Fazio E, Scalese S. Laser processing of TiO_2 colloids for an enhanced photocatalytic water splitting activity. J Colloid Interface Sci 2017;489:131-7.

[12] Fiorenza R, Bellardita M, Barakat T, Scirè S, Palmisano L. Visible light photocatalytic activity of macro-mesoporous TiO_2-CeO_2 inverse opals. J Photochem Photobiol A Chem 2018;352:25-34.

[13] Fiorenza R, Bellardita M, Scirè S, Palmisano L. Effect of the addition of different doping agents on visible light activity of porous TiO_2 photocatalysts. Mol Catal 2018;455:108-20.

[14] Scirè S, Riccobene PM, Crisafulli C. Ceria supported group IB metal catalysts for the combustion of volatile organic compounds and the preferential oxidation of CO. Appl Catal B Environ 2010;101:109-17.

[15] Fiorenza R, Bellardita M, Palmisano L, Scirè S. A comparison between Ccatalytic and photocatalytic oxidation of 2-Propanol over CeO_2 doped TiO_2-based catalysts. J Mol Catal A Chem 2016;415:56-64.

[16] Yan X, Li Y, Xia T. Black titanium dioxide nanomaterials in photocatalysis. Int J Photoenergy 2017;article ID 8529851.

[17] Chen X, Zhao D, Liu K, Wang C, Liu L, Li B, Zhang Z, Shen D. Laser-modified black titanium oxide nanospheres and their photocatalytic activities under visible light. ACS Appl Mater Interfaces 2015;7:16070-7.

[18] Serpone N, Lawless D, Khairutdinov R. Size effects on the photophysical properties of colloidal anatase TiO_2 particles: size quantization versus direct transitions in this indirect semiconductor. J Phys Chem 1995;99:16646-54.

[19] Liqiang J, Yichun Q, Baiqi W, Shudan L, Baojiang J, Libin Y, Wei F, Honggang F, Jiazhong S. Review of photoluminescence performance of nano-sized semiconductor materials and its relationships with photocatalytic activity. Sol Energ Mater Sol C 2006; 90:1773-87.

[20] Lei Y, Zhang LD, Meng GW, Li GH, Zhang XY, Liang CH, Chen W, Wang SX. Preparation and photoluminescence of highly ordered TiO_2 nanowire arrays. Appl Phys Lett 2001;78:1125-7.
[21] Li FB, Li XZ. Photocatalytic properties of gold/gold ion-modified titanium dioxide for wastewater treatment. Appl Catal A Gen 2002;228:15-27.
[22] Yu JG, Yue L, Liu SW, Huang BB, Zhang XY. Hydrothermal preparation and photocatalytic activity of mesoporous Au–TiO_2 nanocomposite microspheres. J Colloid Interface Sci 2009;334:58-64.
[23] Ye Y, Jo C, Jeong I, Lee J. Functional mesoporous materials for energy applications: solar cells, fuel cells, and batteries. Nanoscale 2013;5:4584-605.
[24] Chen JIL, Von Freymann G, Kitaev V, Ozin GA. Effect of disorder on the optically amplified photocatalytic efficiency of titania inverse opals. J Am Chem Soc 2007;129:1196-202.
[25] Sordello F, Duca C, Maurino V, Minero C. Photocatalytic metamaterials: TiO_2 inverse opals. Chem Comm 2011;47:6147-9.
[26] Marcì G, Augugliaro V, Lopez-Munoz MJ, Martın C, Palmisano L, Rives V, Schiavello M, Tilley RJD, Venezia AM. Preparation characterization and photocatalytic activity of polycrystalline ZnO/TiO_2 systems. 1. Surface and bulk characterization. J Phys Chem B 2001;105:1026-32.
[27] Bessekhouad Y, Robert D, Weber JV. Photocatalytic activity of Cu_2O/TiO_2, Bi_2O_3/TiO_2 and $ZnMn_2O_4/TiO_2$ heterojunctions. Catal Today 2005;101:315-21.
[28] Zalfani M, van der Schueren B, Hu ZY, Rooke JC, Bourguiga R, Wu M, Li Y, Tendeloo GV, Su BL. J Mater Chem A 2015;3:21244-56.
[29] Di Paola A, Garcıa-López E, Ikeda S, Marcì G, Ohtani B, Palmisano L. Photocatalytic degradation of organic compounds in aqueous systems by transition metal doped polycrystalline TiO_2. Catal Today 2002;75:87-93.
[30] Asiltürk M, Sayılkan F, Arpac E. Effect of Fe^{3+} ion doping to TiO_2 on the photocatalytic degradation of Malachite Green dye under UV and vis-irradiation. J Photochem Photobiol A 2009;203:64-71.
[31] Bellardita M, García-López E, Marcì G, Nasillo G, Palmisano L. Photocatalytic solar light H_2 production by aqueous glucose reforming. Europ J Inorg Chem 2018;4522-4532.
[32] Wu G, Nishikawa T, Ohtani B, Chen A. Synthesis and characterization of Carbon-doped TiO_2 Nanostructures with Enhanced Visible Light Response. Chem Mater 2007;19:4530-7.
[33] Amadelli R, Samiolo L, Borsa M, Bellardita M, Palmisano L, N-TiO_2 Photocatalysts highly active under visible irradiation for NO_X abatement and 2-propanol oxidation. Catal Today 2013;206:19-25.
[34] Liu Y, Liu J, Lin Y, Zhang Y, Wei Y. Simple fabrication and photocatalytic activity of S-doped TiO_2 under low power LED visible light irradiation. Ceram Int 2009;35:3061-5.
[35] Wang Q, Chen C, Zhao D, Ma W, Zhao J. Change of adsorption modes of dyes on fluorinated TiO_2 and its effect on photocatalytic degradation of dyes under visible irradiation. Langmuir 2008;24:7338-45.
[36] Pikuda O, Garlisi C, Scandura G, Palmisano G. Micro-mesoporous N-doped brookite-rutile TiO_2 as efficient catalysts for water remediation under UV-free visible LED radiation. J Catal 2017;346:109-16.
[37] Ameen S, Akhtar MS, Seo HK, Shin HS. Solution-processed CeO_2/TiO_2 nanocomposite as potent visible light photocatalyst for the degradation of bromophenol dye. Chem Eng J 2014;247:193-8.

[38] Galindo F, Gòmez R, Aguilar M. Photodegradation of the herbicide, 2,4-dichlorophenoxyacetic acid on nanocrystalline TiO_2-CeO_2 sol-gel catalysts. J Mol Catal A Chem 2008;281:119-25.
[39] Lethy KJ, Beena D, Vinod Kumar R, Mahadevan Pillai VP, Ganesan V, Sathe V. Structural, optical and morphological studies on laser ablated nanostructured WO_3 thin films. Appl Surf Sci 2008;254:2369-76.
[40] Yang J, Zhang X, Liu H, Wang C, Liu S, P Sun, Wang L, Liu Y. Heterostructured TiO_2/WO_3 porous microspheres: preparation, characterization and photocatalytic properties. Catal. Today 2013; 201:195-202.
[41] Scholz A, Schnyder B, Wokaun A. Influence of calcination treatment on the structure of grafted WOx species on titania, J Mol Catal A Chem 1999; 138, 249-261.
[42] Su LY, Lu Z. All solid-state smart window of electrodeposited WO_3 and TiO_2 particulate film with PTREFG gel electrolyte. J Phys Chem Solids 1998;59:1175-80.
[43] Vermaire DC, van Berge PC. The Preparation of WO_3/TiO_2 and WO_3/$A1_2O_3$ and characterization by temperature programmed reduction. J Catal 1989;116:309-17.
[44] Kondamareddy KK, Neena D, Lu D, Peng T, Macias Lopez MA, Wang C, Yu Z, Cheng N, Fu DJ, Zhao X. Ultra-trace (parts per million-ppm) W^{6+} dopant ions induced anatase to rutile transition (ART) of phase pure anatase TiO_2 nanoparticles for highly efficient visible light-active photocatalytic degradation of organic pollutants. Appl Surf Sci 2018; 456:676-93.
[45] Sakai K, Hirashita Y, Aihara T, Fukuyama A, Ikari T, Kukita K, Furukawa S. Effect of the molecular weight of a polyethylene glycol on the photoluminescence spectra of porous TiO_2 films for dye-sensitized solar cells, Thin Solid Films 2011;519: 5760-62.
[46] Li XZ, Li FB, Yang CL, Ge WK. Photocatalytic activity of WO_x-TiO_2 under visible light irradiation. J Photochem Photobiol A 2001;141:2209-2217.
[47] Vijayan B, Dimitrijevic NM, Rajh T, Gray KJ. Effect of Calcination Temperature on the Photocatalytic Reduction and Oxidation Processes of Hydrothermally Synthesized Titania Nanotubes. J Phys Chem C 2010;114:12994-13002.
[48] Hurum DC, Agrios AG, Gray KA, Rajh T, Thurnauer MC. Explaining the Enhanced Photocatalytic Activity of Degussa P25 Mixed-Phase TiO_2 Using EPR. J Phys Chem B 2003;107:4545-49.
[49] Naldoni A, Allieta M, Santangelo S, Marelli M, Fabbri F, Cappelli S, Bianchi CL, Psaro R, Dal Santo V. Effect of nature and location of defects on bandgap narrowing in black TiO_2 Nanoparticles. J Am Chem Soc 2012;134:7600-3.
[50] Sinhamahapatra A, Jeon JP, Yu JS. Effect of nature and location of defects on bandgap narrowing in black TiO_2 Nanoparticles. Energ Environ Sci 2015;8:3539-44.
[51] Liu X, Xing Z, Zhang H, Wang W, Zhang Y, Li Z, Wu X, Yu X, Zhou W. Fabrication of 3D mesoporous black TiO_2/MoS_2/TiO_2 nanosheets for visible light driven photocatalysis. ChemSusChem 2016;9:1118-24.
[52] Chen X, Liu L, Yu PY, Mao SS. Increasing Solar Absorption for Photocatalysis with Black Hydrogenated Titanium Dioxide Nanocrystals. Science 2011;331:746-50.
[53] Fiorenza R, Bellardita M, Scirè S, Palmisano L. Photocatalytic H_2 production over Inverse Opal TiO_2 catalysts. Catal Today 2019;321-322:113-19.
[54] Xu H, Chen X, Ouyang SX, Kako T, Ye JH. Size-dependent Mie's scattering effect on TiO_2 spheres for the superior photoactivity of H_2 evolution. J Phys Chem C 2012;116:3833-39.
[55] Chen JIL, Loso E, Ebrahim N, Ozin GA. Synergy of slow photon and chemically amplified photochemistry in platinum nanocluster-loaded Inverse Titania Opals. J Am Chem Soc 2008;130:5420-21.

[56] Bamwenda GR, Arakawa H. The photoinduced evolution of O_2 and H_2 from a WO_3 aqueous suspension in the presence of Ce^{4+}/Ce^{3+}. Sol Energy Mater Sol Cells 2001;70:1-14.
[57] Lai CW, Sreekantan S. Incorporation of WO_3 species into TiO_2 nanotubes via wet impregnation and their water-splitting performance. Electrochim Acta 2013;87:294-302.
[58] Tong H, Chen Q, Zhao L, Wu D, Yang D, Photo-catalytic behavior of WO_3-TiO_2 catalysts with oxygen evolution. Integr Ferroelectr 2011;127:63-70.
[59] Li C, Jiang Z, Yao Z. Fabrication and characterization of multi-metal co-doped titania films for a water-splitting reaction. Dalton Trans 2010;39:10692-96.
[60] Sajjad AKL, Shamaila S, Tian BZ, Chen F, Zhang JL. One step activation of WO_x/TiO_2 nanocomposites with enhanced photocatalytic activity. Appl Catal B Environ 2009;91:397-405.
[61] Yang XL, Dai WL, Guo CW, Chen H, Cao Y, Li HX, He HY, Fan KN. Synthesis of novel core-shell structured WO_3/TiO_2 spheroids and its applications in the catalytic oxidation of cyclopentene to glutaraldehyde by aqueous H_2O_2. J Catal 2005;234:438-50.

Caption to figures

Fig. 1 Characterization data of TiO_2, Macro TiO_2 and TiO_2 LT samples. (A) Raman spectra; (B) Raman map of TiO_2 LT sample showing in blue the signal at 145 cm^{-1} for anatase phase and in red that at 445 cm^{-1} for rutile; (C) PL spectra for TiO_2, Macro TiO_2 and TiO_2 LT materials respectively.

Fig. 2 H_2 production over TiO_2, TiO_2 LT and Macro TiO_2 samples: (A) under UV lamp; (B) under solar lamp.

Fig. 3 SEM images of macroporous TiO_2-based photocatalysts (Macro-TiO_2, Macro TiO_2-CeO_2 and Macro TiO_2-W).

Fig. 4 Characterization data of TiO_2 and macroporous TiO_2-based photocatalysts. (A) Raman spectra, (B) PL spectra.

Fig. 5 H_2 production over TiO_2, TiO_2-CeO_2 and TiO_2-W photocatalysts: (A) under UV lamp; (B) under solar lamp.

Fig. 6 H_2 production over macroporous TiO_2-based photocatalysts: (A) under UV lamp; (B) under solar lamp.

Fig. 7 General comparison of H_2 production by photocatalytic water splitting over TiO_2-based catalysts used in this work: (A) under UV lamp; (B) under solar lamp.

Table 1 BET Surface area and band-gap energies (E_g) for investigated TiO_2-based samples.

Catalysts	**S_{BET} ($m^2 g^{-1}$)**	**E_g(eV)**
TiO_2	55.0	3.24
TiO_2 LT	61.1	3.23
TiO_2-CeO_2	57.5	3.19
TiO_2-W	56.1	3.25
Macro TiO_2	28.3	3.23
Macro TiO_2-CeO_2	23.3	3.18
Macro TiO_2-W	28.8	3.26

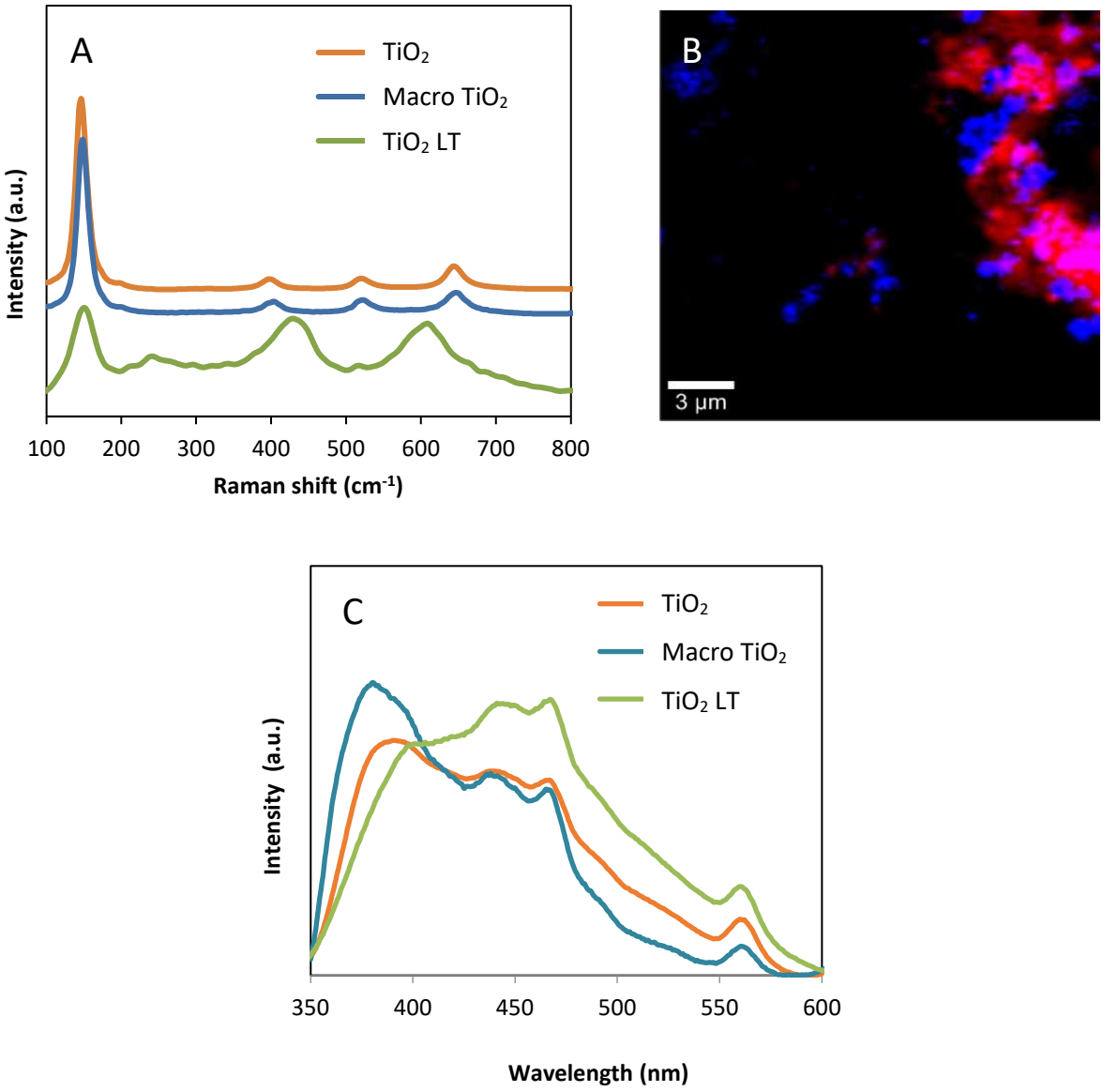
A
TiO2
Macro TiO2
TiO2 LT
Intensity (a.u.)
100
200
300
400
500
600
700
800
Raman shift (cm-1)
B
3 µm
C
TiO2
Macro TiO2
TiO2 LT
Intensity (a.u.)
350
400
450
500
550
600
Wavelength (nm)

Fig. 1

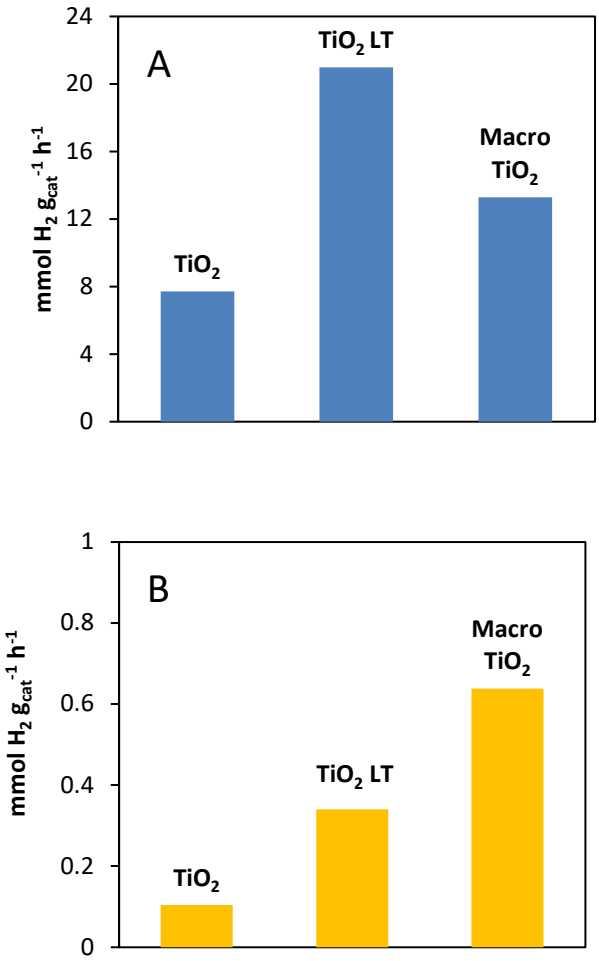
A
B
mmol H2 gcat-1 h-1
TiO2
TiO2 LT
Macro TiO2
0
4
8
12
16
20
24
0.2
0.4
0.6
0.8
1

Fig. 2

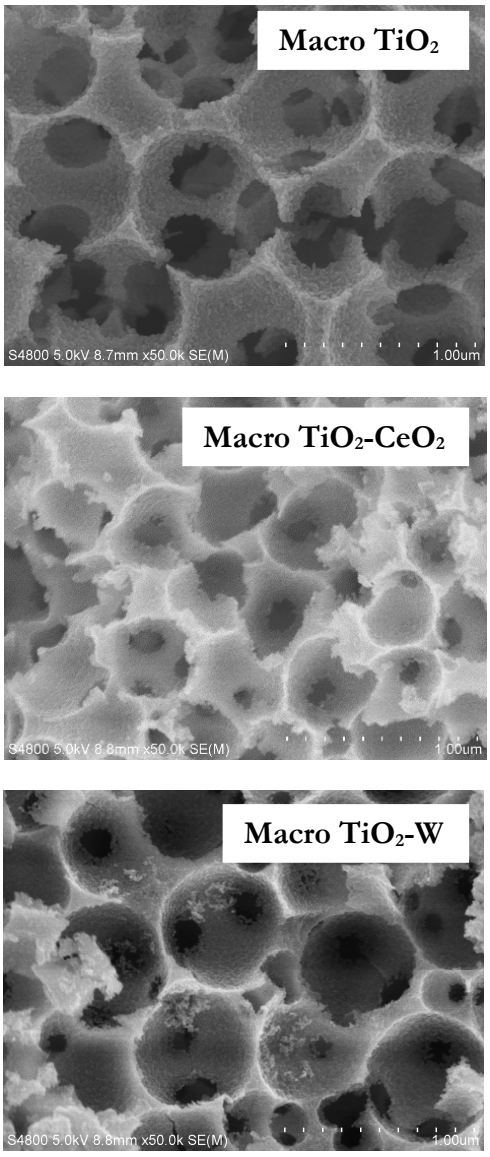
Macro TiO_2
S4800 5.0kV 8.7mm x50.0k SE(M)
1.00um
Macro TiO_2-CeO_2
S4800 5.0kV 8.8mm x50.0k SE(M)
1.00um
Macro TiO_2-W
S4800 5.0kV 8.8mm x50.0k SE(M)
1.00um

Fig. 3

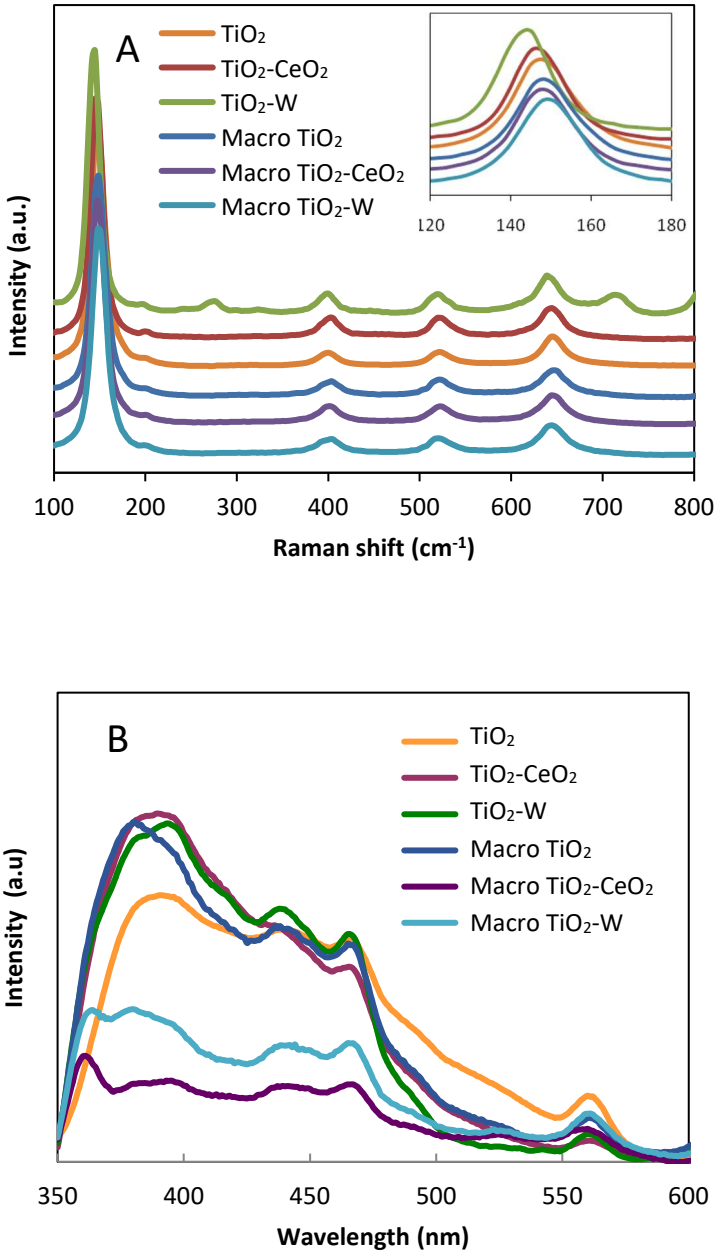
A
TiO2
TiO2-CeO2
TiO2-W
Macro TiO2
Macro TiO2-CeO2
Macro TiO2-W
Intensity (a.u.)
100
200
300
400
500
600
700
800
Raman shift (cm-1)
120
140
160
180
B
TiO2
TiO2-CeO2
TiO2-W
Macro TiO2
Macro TiO2-CeO2
Macro TiO2-W
Intensity (a.u)
350
400
450
500
550
600
Wavelength (nm)

Fig. 4

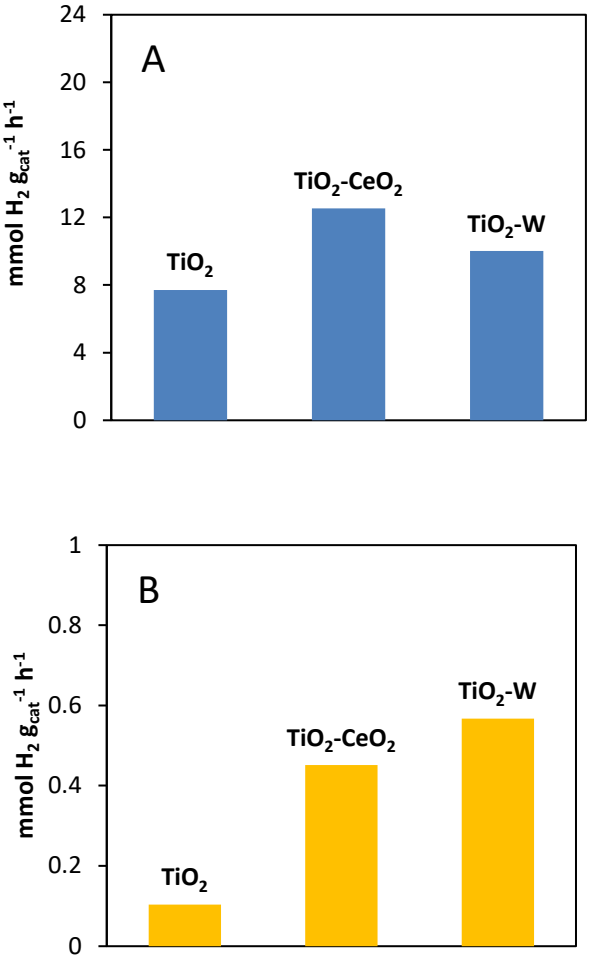
A
mmol H_2 g_{cat}^{-1} h^{-1}
24
20
16
12
8
4
0
TiO_2
TiO_2-CeO_2
TiO_2-W
B
mmol H_2 g_{cat}^{-1} h^{-1}
1
0.8
0.6
0.4
0.2
0
TiO_2
TiO_2-CeO_2
TiO_2-W

Fig. 5

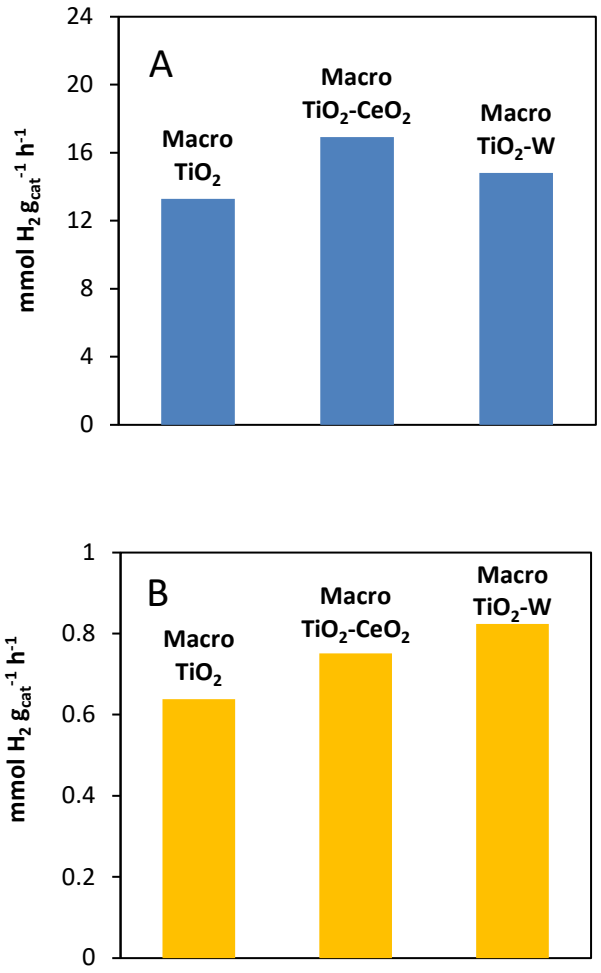
A
Macro TiO2
Macro TiO2-CeO2
Macro TiO2-W
mmol H2 gcat -1 h-1
24
20
16
12
8
4
0
B
Macro TiO2
Macro TiO2-CeO2
Macro TiO2-W
mmol H2 gcat -1 h-1
1
0.8
0.6
0.4
0.2
0

Fig. 6

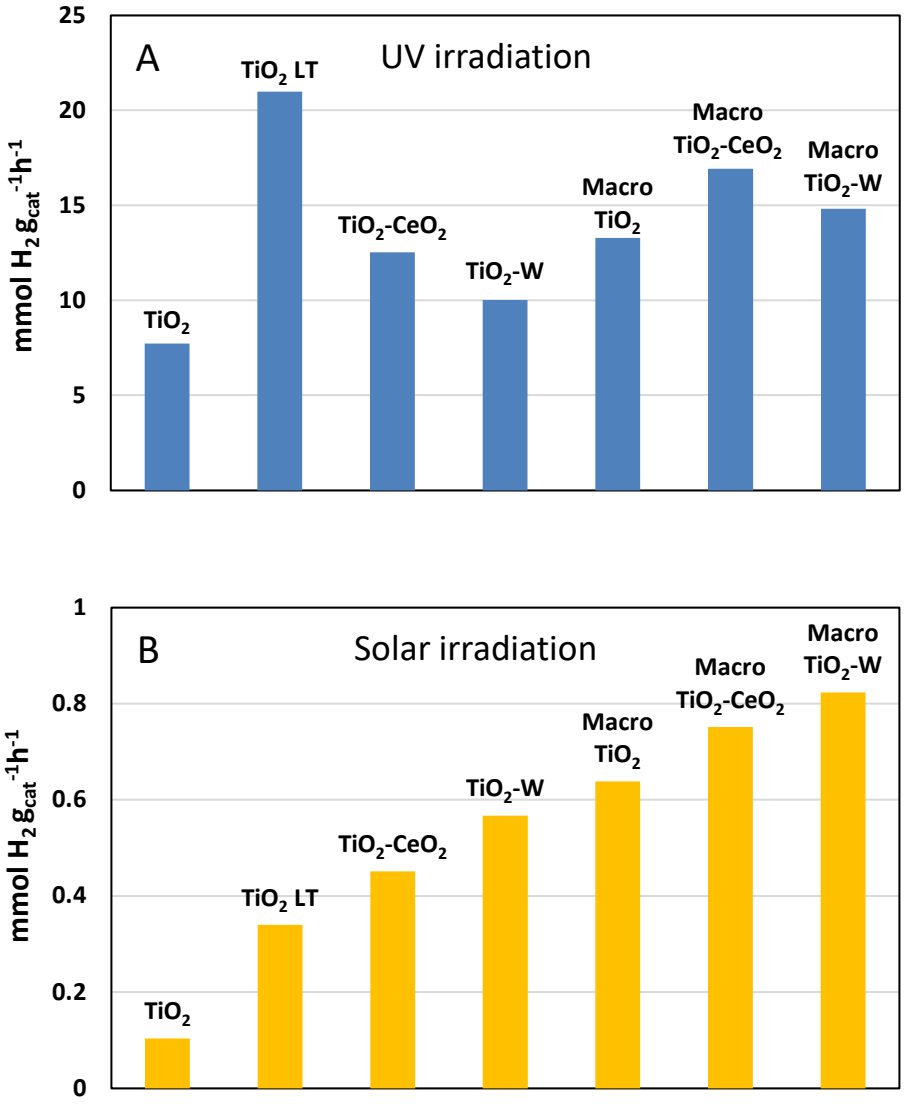
A
UV irradiation
mmol $H_2 g_{cat}^{-1} h^{-1}$
25
20
15
10
5
0
TiO_2
TiO_2 LT
TiO_2-CeO_2
TiO_2-W
Macro TiO_2
Macro TiO_2-CeO_2
Macro TiO_2-W
B
Solar irradiation
mmol $H_2 g_{cat}^{-1} h^{-1}$
1
0.8
0.6
0.4
0.2
0
TiO_2
TiO_2 LT
TiO_2-CeO_2
TiO_2-W
Macro TiO_2
Macro TiO_2-CeO_2
Macro TiO_2-W

Fig. 7